(PDGF) receptor-β (PDGFRB) and *PDGFB* have recently been reported to cause calcification in the brain.[14,15]

We have collected clinical information of patients with IBGC in a nationwide survey in Japan. Here, on the basis of a mutational analysis of *SLC20A2*, we aim to establish the molecular epidemiology of IBGC3 and evaluate clinically and genetically *SLC20A2* mutations in Japan.

METHODS **Subjects and samples.** We collected clinical information on patients with IBGC in a nationwide study. The criteria for the selection of patients in the initial survey were as follows: 1) conspicuous calcification is observed in the basal ganglia and/or dentate nucleus by CT scan; 2) calcification is bilateral and symmetrical; and 3) idiopathic (absence of biochemical abnormalities, and an infectious, toxic, or traumatic cause).[2,3] Neurologists enrolled patients in the survey. They examined the medical charts and performed the neurologic examinations again if necessary. The survey was approved by the Ethics Committee of the Gifu University Graduate School of Medicine. During the survey, some patients were found to have hypoparathyroidism, Aicardi-Goutières syndrome, and Cockayne syndrome, and these patients were excluded. For the genetic study, a total of 69 subjects from 41 hospitals provided written informed consent and were enrolled in the project. Of these patients, 46 came from families with a single affected member, and the other 23 came from 10 families with multiple affected members. We defined the former as sporadic patients and the latter as familial patients. The patients' mean age ± SD was 41.3 ± 23.6 years at registration. The patients comprised 32 males and 37 females.

Standard protocol approvals, registrations, and patient consents. All experiments on human DNA were approved by the Ethics Committees of both Gifu University and the University of Tokyo. After written informed consent was obtained, peripheral blood samples were collected.

Mutational analysis. Genomic DNA was extracted from the whole blood samples. *SLC20A2* analysis was performed by Sanger sequencing of all coding regions, as described in detail in e-Methods and table e-1, A and B, on the *Neurology*® Web site at www.neurology.org. The pathologic potential of the identified variants was predicted using PolyPhen-2 (http://genetics.bwh.harvard.edu/pph/).[16]

RESULTS **Mutational analysis.** We screened a total of 69 subjects including 23 subjects from 10 families in which multiple affected subjects were observed and 46 subjects in sporadic cases, all of whom were Japanese. Six new mutations in *SLC20A2* were found: 4 missense mutations, 1 nonsense mutation, and 1 frameshift mutation (figure 1). Electropherograms showed the individual heterozygous mutations (figure e-1). None of them were present in an in-house exome sequencing data set (358 Japanese control subjects), dbSNP 137 (www.ncbi.nlm.nih.gov/snp/), or the National Heart, Lung, and Blood Institute "Grand Opportunity" Exome Sequencing Project (ESP6500SI-V2). In silico analysis predicted deleterious consequences, as determined from the residue changes in figures 1 and e-1. When confined to the FIBGC patients, 5 of the 10 families (50.0%) showed mutations in *SLC20A2*. In contrast, 2 of the 46 patients (4.3%) with sporadic IBGC carried mutations in *SLC20A2* in this study.

Clinical manifestations. The clinical manifestations are summarized in table 1. A positive family history of IBGC was present in 5 families. Families 1 and 2 had the same mutation.

Familial cases. ***Case 1 (in family 1).*** The proband in family 1 was a 64-year-old woman who had dysarthria and gait disturbance for 5 years. She showed no dementia. Her neurologic examination revealed dysarthria, small steppage gait, rigidity at bilateral wrist joints, bradykinesia, and a pyramidal sign. Her CT images revealed severe calcification at the bilateral globus pallidus, caudate nuclei, thalamus, subcortical white matter, and dentate nuclei (figure 2C). Her son's CT showed similar brain calcification (figure 2D), although he was clinically asymptomatic. His DNA study revealed the

Figure 1 **Schematic representation of causative mutations in *SLC20A2* in idiopathic basal ganglia calcification**

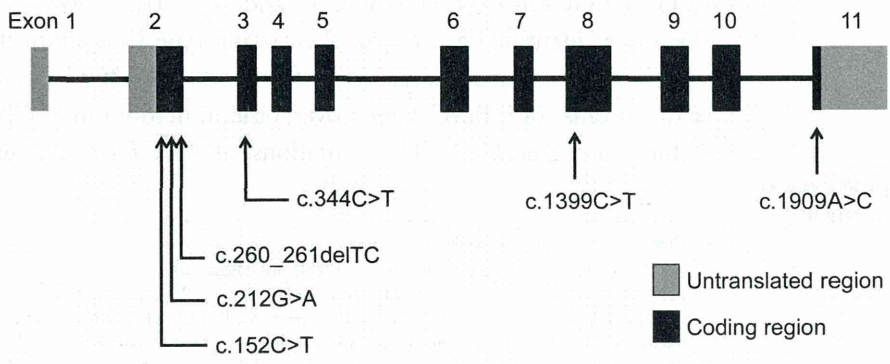

Six new causative mutations in exon 2 (c.152C>T, c.212 G>A, c.260_261delTC), exon 3 (c.344C>T), exon 8 (c.1399C>T), and exon 11 (c.1909A>C) were found in this study.

Table 1 Clinical features of 6 individuals (probands) with *SLC20A2* mutations

	Case 1	Case 2	Case 3	Case 4	Case 5	Case 6	Case 7
Mutation	c.1909A>C	c.1909A>C	c.344C>T	c.212G>A	c.1399C>T	c.152C>T	c.260_261delTC
	S637R	S637R	T115M	R71H	R467X	A51V	L87Hfs*6
Zygosity	Hetero	Hetero	Hetero	Hetero	Hetero	Hetero	Hetero
Exon	11	11	3	2	8	2	2
Proband information							
Age at detection of calcification, y	60	51	60	73	23	71	74
Age at onset, y	58	50	60	71	15	71	57
Onset symptom	Dysarthria	Dysarthria	Dementia	Parkinsonism	PKC	Dementia	Athetosis
Neurologic findings							
Cognitive impairment (MMSE)	27	24	20	16	30	22	22
Pyramidal sign	+	+	−	−	−	−	−
Extrapyramidal sign	+	+	−	+	−	−	+
Family information (except the proband)							
No. of other individuals with calcification	1	2	5	1	1	0[a]	0[a]
No. of other individuals with confirmed mutations	1	NE	5	NE	1	NA	NA
No. of other symptomatic individuals	0	0	2	0	0	NA	NA
Other symptoms (no.) in the family	—	—	Mental disorder (1), alcoholism (1)	—	—	NA	NA

Abbreviations: MMSE = Mini-Mental State Examination; NA = not applicable; NE = not examined; PKC = paroxysmal kinesigenic choreoathetosis.
[a] Because there was no other family member who had any neurologic symptoms, brain CT screening of other family members was not performed.

same mutation in exon 11 that had been found in his mother.

Case 2 (in family 2). The proband in family 2 was a 54-year-old woman who had dysarthria and gait disturbance for 4 years. She showed mild mental deterioration in Mini-Mental State Examination (MMSE) score of 24 points, frontal signs, dysarthria, mild parkinsonism (rigidity of bilateral wrist joints and bradykinesia), adiadochokinesis, spasticity, and small steppage gait. Her CT images revealed severe calcification at the bilateral globus pallidus, caudate nuclei, thalamus, subcortical white matter, and dentate nuclei (figure 2E). Although her son and cousin also showed calcification in CT images, they were asymptomatic. Her DNA analysis revealed the same mutation as that in family 1.

Case 3 and other symptomatic individuals (in family 3). The proband was a 69-year-old woman (II-1 in the pedigree in figure 3). She was admitted to a hospital at the age of 65 because of forgetfulness since the age of 60 years. Her MMSE score was 20, which indicated a possibility of dementia (MMSE score below 22). Decreased blood flow was detected in the bilateral basal ganglia and thalamus and the right frontal lobe in particular by SPECT. She had a positive family history of brain calcification, as shown in figure 3A. The initial clinical diagnosis had been diffuse neurofibrillary tangles with calcification (DNTC),[17] although to our knowledge familial cases of DNTC have not been reported. Her son had psychological disorders including violent behavior; unfortunately, no brain CT had yet been performed on him. In the patients in family 3, the degree of calcification was mild compared with that observed in the other families (figure 3, B–G). Her brother with calcification in the brain (II-7) had a mental disorder and another (II-8) presented with alcoholism. The 3 other relatives with calcification were asymptomatic (II-5, II-9, and III-3). The symptomatic patients (II-1, II-7, and II-8) showed more apparent brain atrophy than the others (figure 3, B, D, and E, respectively). The individuals with calcification on the CT images (II-1, II-5, II-7, II-8, II-9, and III-3) had the same mutation in exon 3 in *SLC20A2*. However, the individuals with no calcification (III-2, III-5, and IV-1) revealed no mutation in *SLC20A2*. In summary, 6 patients had calcification among the 10 individuals examined by CT scan in family 3 and all of them carrying the *SLC20A2* mutation exhibited similar calcification on CT images. However, persons without the mutation did not show calcification.

Case 4 (in family 4). Family 4 had a mutation in exon 2. The proband developed clumsiness of her hands and gait unsteadiness at the age of 71 years, and she was diagnosed as having Parkinson disease. Visual

Figure 2 CT images and family trees of families 1 and 2

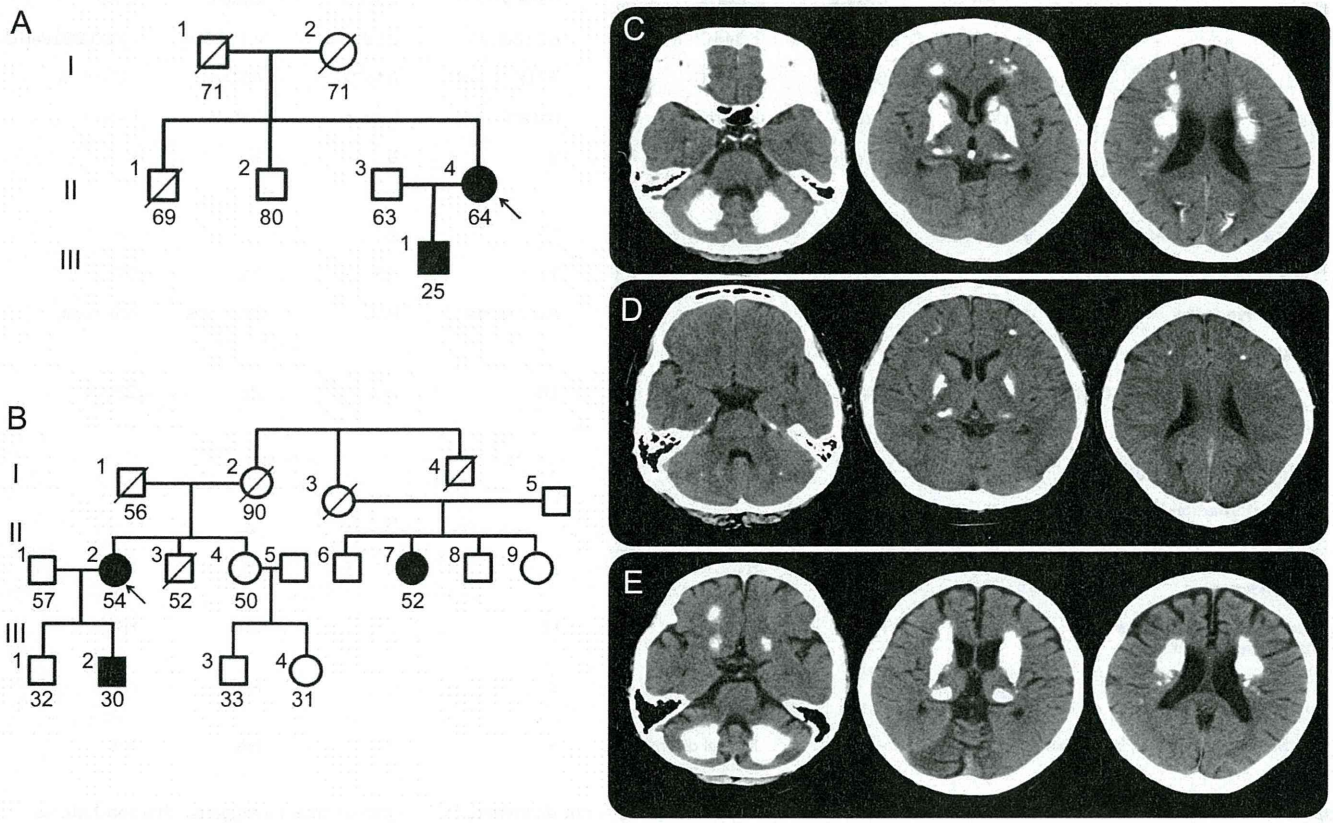

(A) Family tree of family 1. (B) Family tree of family 2. The arrow indicates the index subject. Filled symbols represent patients affected by brain calcification. We show the ages of persons under symbols in the family tree for those we could obtain. (C) CT images of proband (II-4 in pedigree of family 1, part A). (D) CT images of the proband's son (III-1 in pedigree of family 1, part A). (E) CT images of the proband (II-2 in pedigree of family 2, part B). All have mutation of S637R.

hallucinations started with the initiation of medication. She showed parkinsonism (rigidity, bradykinesia, and postural instability), which responded to levodopa. Her MMSE score was 16. Her brain CT images revealed calcification at the globus pallidus, caudate nuclei, and dentate nuclei, and her daughter, who was asymptomatic, also had intracranial calcification (figure e-2C). Brain CT was not performed in her other children. Her SPECT images showed decreased perfusion in the bilateral frontal, temporal, and parietal regions of the brain. She died of pneumonia at the age of 79. Neuropathologic examination revealed neuronal loss and Lewy bodies in the substantia nigra, locus ceruleus, amygdala, and parahippocampal gyrus indicative of Parkinson disease, and prominent deposition of calcium in the parenchyma and the wall of arteries in the globus pallidum and dentate nuclei compatible with the pathologic findings of IBGC.

Case 5 (in family 5). The proband was a 24-year-old man who had paroxysmal kinesigenic choreoathetosis (PKC). His laboratory data were normal except for CT findings. He presented with an attack of PKC after exercise and his symptom responded well to carbamazepine. His CT images revealed calcification at the globus pallidus, thalamus, subcortical white matter, and dentate nuclei (figure e-2B [A]). We had an opportunity to examine his parents, who had no symptoms or signs. Mutational analysis of *SLC20A2* of his parents with their informed consent revealed the same mutation in exon 8 in his mother as he had. Brain CT scan of his mother confirmed calcification at the globus pallidus, subcortical white matter, and dentate nuclei.

Sporadic cases. ***Case 6.*** The patient had a mutation in exon 2. She was a 72-year-old woman who noticed forgetfulness at the age of 71. She had no motor deficits. Her MMSE score was 22, and her score on the revised Hasegawa Dementia Scale was 24. Her Frontal Assessment Battery score at bedside was 5, indicating a frontal lobe deficit (cutoff score, 11/12). The index scores of the revised Wechsler Memory Scale were as follows: attention and concentration, 86; verbal memory, 89; general memory, 85; attention/concentration, 71; and delayed recall, 75. Her brain CT images revealed calcification at the globus pallidus, caudate nuclei, thalamus, subcortical and periventricular white matter, and dentate nuclei (figure e-2B [B]). Her SPECT images showed decreased perfusion in the left frontal,

Figure 3 Pedigree and CT images of family 3

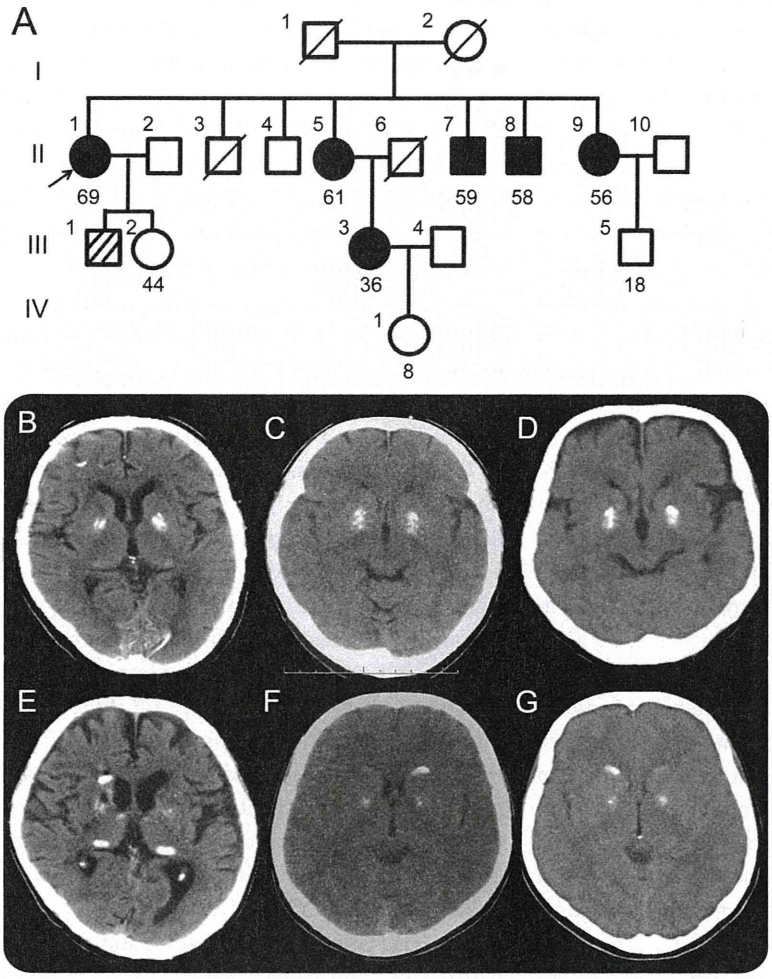

(A) Pedigree of family 3. The arrow indicates the index subject. Filled symbols represent patients affected by brain calcification. We show the ages of persons under symbols in the family tree for those we could obtain. The striped symbol represents a symptomatic patient, although his CT image and DNA sample were not available for the study. (B) CT image of the proband (II-1 in pedigree of family 3). (C) CT image of asymptomatic II-5. (D) CT image of symptomatic II-7. (E) CT image of symptomatic II-8. (F) CT image of asymptomatic II-9. (G) CT image of asymptomatic III-3. All have mutation of T115M.

temporal, and parietal regions of the cerebrum and bilateral cerebellum. [^{11}C] Pittsburgh compound B (PiB) retention was not observed by [^{11}C]PiB PET. There were no other family members presenting with similar neurologic symptoms. CT scan was not performed for other individuals in the family.

Case 7. The patient was a 78-year-old man who had a frameshift in exon 2. Involuntary movement of the left thumb and index finger like "pill-rolling" began in his sixth decade. His family first noticed memory impairment at the age of 75. Gait disturbance appeared at the age of 77 and oral dyskinesia and left shoulder shrugging appeared at the age of 78. His scores on the MMSE and Frontal Assessment Battery were 22 and 10, respectively. His brain CT images showed calcification at the globus pallidus, thalamus, subcortical and periventricular white matter, and dentate nuclei (figure e-2B [C]). His SPECT images showed decreased perfusion in the bilateral (predominantly in the left) frontal and temporal regions of the cerebrum and bilateral cerebellum. [^{11}C]PiB retention was not observed by [^{11}C]PiB PET, which was performed at the age of 81. There were no other family members presenting with similar neurologic symptoms. CT scan was not performed for other individuals in the family.

DISCUSSION We have obtained clinical information of 161 patients with brain calcification in a nationwide study. We discovered that 3 patients had hypoparathyroidism, Aicardi-Goutières syndrome, and Cockayne syndrome during the survey. CT images revealed varying degrees of calcification, from marked calcification in the basal ganglia to patchy calcification in various regions, suggesting diversity in the etiologies. Some patients were incidentally found to have calcification by CT performed for head injury caused by accidents. Because our previous survey revealed a considerable frequency (1%–2%) of patchy calcification in the CT images of all patients in 2 university hospitals in Japan,[18] more asymptomatic IBGC patients with patchy calcification may exist than the number that we had previously assumed to be present in the population in Japan. After the examination by neurologists, we collected 69 DNA samples from patients who met the criteria for IBGC.[2,3] Symptoms and neurologic findings varied widely from asymptomatic to variable symptoms including headaches, psychosis, and dementia.

In this study, we investigated mutations in *SLC20A2* in 69 patients with IBGC in Japan and identified 4 new mutations in 10 familial cases (the same mutation in 2 families) and 2 other new mutations in 46 sporadic cases. The frequency of families with mutations in *SLC20A2* was 50% (5 of the 10 families), and that of sporadic patients was 4.3% (2 of the 46 patients). The frequency of the mutations in *SLC20A2* in FIBGC in Japan was as high as in other countries in a previous report.[10] Case 5 indicates that it is difficult to reliably determine sporadic cases without brain CT scans and genetic studies of all members in the family.

The mutations in our study existed in exons 2, 3, 8, and 11. One of these mutations (R467X) in exon 8 resulted in a substitution to a TGA stop codon, and the other (c.260_261delTC) in exon 2 was a frameshift. None of the mutations were reported previously, indicating heterogeneities of the mutations in *SLC20A2*. Taken together with other reports, causative mutations identified in *SLC20A2* include 6 mutations in exon 2, 1 in exon 3, 3 in exon 4, 1 in exon 5, 1 in exon 7, 10 in exon 8, 2 in exon 9, 4 in exon 10, and 4 in exon 11.[9–12] It does not seem that there

are mutation hot spots in *SLC20A2*. The in silico analysis using PolyPhen-2 for the missense mutations predicted all to be likely damaging, as determined from the residue changes. We drew the structure model of the PiT-2 protein using the TOPO2 software (http://www.sacs.ucsf.edu/TOPO/top.html). The schematic structure of the PiT-2 protein with the mutations is shown in figure 4.

Although the clinical features varied widely among the families with IBGC with *SLC20A2* mutations, the patients in families 1 and 2 with the same *SLC20A2* mutation exhibited similar clinical manifestations including dysarthria, mild cognitive decline, pyramidal signs, and extrapyramidal signs as well as similar ages at detection of calcification and onset of symptoms. Of note, the CT images among the affected individuals in the 2 families are similar (figure 2). In family 3, in contrast, 3 symptomatic patients presented with dementia, psychological disorder, and alcoholism, accompanied with brain atrophy in CT images. None of them showed movement disorders such as those in families 1 and 2.

Although mutational analysis and CT scan were not performed in other familial members of cases 6 and 7, concordance of the presence of mutations of *SLC20A2* and brain calcification were confirmed in 15 individuals, and we did not observe any individuals who carried the mutation and did not show brain calcification. These observations strongly support a high penetrance of the *SLC20A2* mutations regarding brain calcification.

Correlations of genotypes and neurologic phenotypes, however, have been controversial. *SLC20A2* mutations in patients with FIBGC have been described to show variability in clinical manifestations among the families. In the present study, the 2 affected individuals in families 1 and 2, who carried the same mutation, exhibited quite similar neurologic manifestations and clinical courses, suggesting a genotype-phenotype correlation of the S637R mutation. Of note, 2 individuals aged 56 and 61 years in family 3 did not exhibit any neurologic manifestations despite carrying the mutation and having brain calcification, indicating that penetrance regarding the neurologic manifestations is incomplete.

In case 4, interestingly, the proband showed pathologic findings of both IBGC and Parkinson disease. Because Parkinson disease is a common disorder in aged people, there remains a possibility that the presence of IBGC and Parkinson disease is coincidental.

Case 5 had a mutation that leads to a premature stop codon, making an incomplete structure of PiT-2. His neurologic symptom was PKC controllable by carbamazepine. Intriguingly, several patients with IBGC have been reported to present with PKC or paroxysmal nonkinesigenic dyskinesia.[19,20] For these cases of PKC or paroxysmal nonkinesigenic dyskinesia, mutational analyses of not only *SLC20A2* but also *PRRT2* and MRI will be indispensable.[21,22]

Herein, we have reported 5 cases of FIBGC and 2 cases of IBGC with *SLC20A2* mutations in Japan. We could not find any characteristic features of Japanese patients, although we had discovered that each case has a new mutation in *SLC20A2*, respectively.

The mechanisms of calcification and cell damage remain to be elucidated. Despite that the expression of PiT-2 encoded by *SLC20A2* is distributed widely in the human body,[23] mutations in *SLC20A2* cause

Figure 4 **Schematic structure of PiT-2 (type III sodium-dependent phosphate transporter) with the mutations**

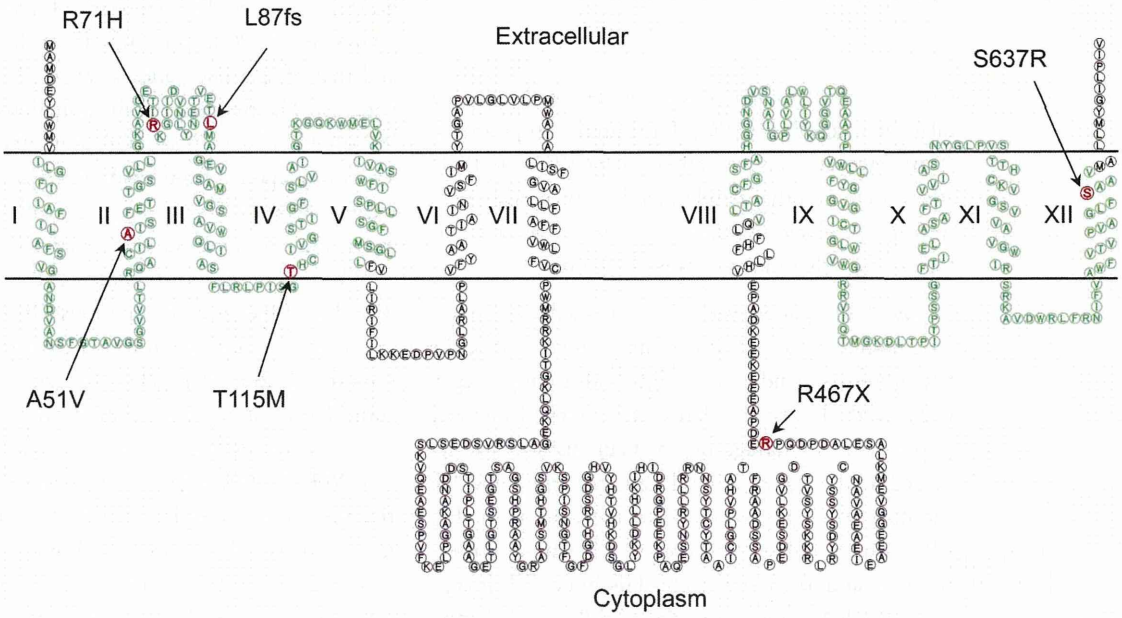

calcification only in the brain. Mutations in *SLC34A2* have been reported to cause pulmonary alveolar microlithiasis.[24] Because Npt2b encoded by *SLC34A2* is the only phosphate transporter that is highly expressed in the lungs,[25] the mutations in *SLC34A2* are compatible with the lesion of the alveolar type II cells in the lungs.[24] Because the limitation of calcification to the brain cannot be explained by only the mutation in *SLC20A2* followed by abnormalities of inorganic phosphate (Pi) transport via PiT-2, there might be some other genes responsible for calcification in the brain, or the mutations in *SLC20A2* may take some toxic gain of function. The dysfunction of Pi transport can explain the accumulation of various metals in regions of the brain and the abnormal distribution of metals, which we observed in CSF[26] and hair in the patients with IBGC.[27] We have recently shown that PiT-2 immunopositivity was expressed predominantly in neurons, astrocytes, and vascular endothelial cells in the mouse brain.[28] PDGF-B is expressed in endothelial cells and neurons.[29] PDGF-B homodimer (PDGF-BB) enhanced the expression of PiT-1 mRNA encoded by *SLC20A1* in human aortic smooth muscle cells.[30] The hypomorph of PDGF-B in mice has recently been revealed to cause brain calcification through pericyte and blood-brain barrier impairment.[15] Recently, simple knockout of *SLC20A2* has also been shown to lead to calcification in the mouse brain.[31] PiT-2, PDGF, and as yet undetermined other molecules are considered to have pivotal roles in blood vessel–associated calcification and neuronal death in patients with IBGC. Elucidation of the molecular basis underlying IBGC will contribute to the development of therapeutic measures for patients with calcification in the brain.

AUTHOR CONTRIBUTIONS

Principal investigator: Isao Hozumi. Study supervision: Shoji Tsuji, Gen Sobue, Takashi Inuzuka, and Kortaro Tanaka. Manuscript draft preparation: Megumi Yamada and Masaki Tanaka. Acquisition and collection of data: Seiju Kobayashi, Yoshiharu Taguchi, Shutaro Takashima, Tetsuo Touge, Hiroyuki Hatsuta, and Shigeo Murayama. Analysis and interpretation: Megumi Yamada, Masaki Tanaka, Mari Takagi, Yuichi Hayashi, Masayuki Kaneko, Naoki Atsuta, Nobuyuki Shimozawa, Hiroyuki Ishiura, and Jun Mitsui.

ACKNOWLEDGMENT

The authors thank the patients and their families who supported this research. The authors also thank Societas Neurologica Japonica and the Japanese Society of Child Neurology (Professor Hideo Sugie, Jichi Medical University) for cooperation of collecting patients. The authors thank the Japanese Consortium for Amyotrophic Lateral Sclerosis research (JaCALS) and Japan MSA research consortium (JAMSAC) for kindly providing the exome sequencing data of controls.

STUDY FUNDING

This study was sponsored by a grant from the Ministry of Health, Labour and Welfare of Japan (H23-Nanbyo-Ippan-106 and H25-Nanchitoh [Nan]-Ippan-002).

DISCLOSURE

M. Yamada, M. Tanaka, and M. Takagi report no disclosures. S. Kobayashi received research funds from Research Funding Shionogi Pharma Inc., Mochida Pharmaceutical Co., Ltd., and Eli Lilly Japan K.K. Y. Taguchi and S. Takashima report no disclosures. K. Tanaka received funds from the University of Toyama, Otsuka Pharmaceutical Co., Ltd., Mochida Pharmaceutical Co., Ltd., Sanofi Co., Ltd., GlaxoSmithKline Co., Ltd., and Nippon Boehringer Ingelheim Co., Ltd. T. Touge reports no disclosures. H. Hatsuta received a fund from the Ministry of Education, Culture, Sports, Science and Technology of Japan (Grant-in-Aid for Young Scientists [B] 24700371). S. Murayama received research funds from the Ministry of Education, Culture, Sports, Science and Technology of Japan (Grants-in-Aid for Comprehensive Scientific Research Network for Brain Bank; Basic Research B for Parkinson Disease), National Center for Geriatrics and Gerontology (Brain Bank), the Ministry of Health, Labour and Welfare of Japan (Grant-in-Aid for Neurodegenerative Disease, Prion Disease and Amyotrophic Lateral Sclerosis), and National Center for Neurology and Psychiatry (Brain Bank). Y. Hayashi reports no disclosures. M. Kaneko received funds from the Ministry of Education, Culture, Sports, Science and Technology of Japan (Grant-in-Aid for Young Scientists [B] 23790095, Grant-in-Aid for Scientific Research on Priority Areas 22020032, and Grant-in-Aid for Scientific Research [B] 21300142), Takeda Science Foundation, the Research Foundation for Pharmaceutical Sciences, Niigata Brain Institute, and Japan Amyotrophic Lateral Sclerosis Association. H. Ishiura received funds from the Ministry of Education, Culture, Sports, Science and Technology of Japan (Grant-in-Aid for Young Scientists [Start-up] 24890044) and the Cell Science Research Foundation. J. Mitsui received a fund from the Ministry of Education, Culture, Sports, Science and Technology of Japan (Grant-in-Aid for Young Scientists [B] 25860700). N. Atsuta is funded by Grants-in-Aid for Scientific Research from the Ministry of Education, Culture, Sports, Science and Technology (MEXT) of Japan (grant number 25461277) and the Inochinoiro Foundation of Japan. G. Sobue serves on the scientific advisory board for the Kanae Science Foundation for the Promotion of Medical Science, Takeda Science Foundation, and serves as an advisory board member of *Brain*, an editorial board member of *Degenerative Neurological and Neuromuscular Disease*, the *Journal of Neurology*, and *Amyotrophic Lateral Sclerosis and Frontotemporal Degeneration*, and is funded by the Ministry of Education, Culture, Sports, Science and Technology of Japan; the Ministry of Welfare, Health and Labor of Japan; the Japan Science and Technology Agency, Core Research for Evolutional Science and Technology. N. Shimozawa reports no disclosures. T. Inuzuka received research funds from the Ministry of Health, Labour and Welfare of Japan (H23-Nanbyo-Ippan-106, H22-Nanbyo-Shitei-002, H23-Nanbyo-Shitei-001, H23-Nanti-Ippan-039), and the Ministry of Education, Culture, Sports, Science and Technology of Japan (Basic Research [C] 24591256), and Eizai Co., Ltd., Dainippon Sumitomo Pharmaceutical Co., Ltd., Takeda Pharmaceutical Co., Ltd., Otsuka Pharmaceutical Co., Ltd., and GlaxoSmithKline, LSE: GSK, NYSE: GSK. S. Tsuji received research funds from the Ministry of Education, Culture, Sports, Science and Technology of Japan (Grants-in-Aid for Scientific Research on Innovative Areas [22129001 and 22129002]), the Ministry of Health, Labour and Welfare of Japan (Grant-in-Aid H23-Jitsuyoka [Nanbyo]-Ippan-004), Sanofi K.K., Japan Blood Products Organization, Mitsubishi Tanabe Pharma Co., Pfizer Japan Inc., Ono Pharmaceutical Co., Ltd., Daiichi Sankyo Co., Ltd., Eisai Co., Ltd., Kowa Pharmaceutical, Co., Ltd., and GlaxoSmithKline, K.K. I. Hozumi received funds from the Ministry of Health, Labour and Welfare of Japan, the Ministry of Education, Culture, Sports, Science and Technology of Japan (Basic Research [C] 24590664), Niigata Brain Institute, the Community for Communication of Technology of Gifu University, and Eizai Co., Ltd. Go to Neurology.org for full disclosures.

Received May 18, 2013. Accepted in final form November 15, 2013.

REFERENCES

1. Manyam BV. What is and what is not "Fahr's disease." Parkinsonism Relat Disord 2005;11:73–80.

2. Bonazza S, La Morgia C, Martinelli P, Capellari S. Striopallido-dentate calcinosis: a diagnostic approach in adult patients. Neurol Sci 2011;32:537–545.
3. Sobrido MJ, Hopfer S, Geschwind DH. Familial idiopathic basal ganglia calcification. In: GeneReviews NCBI Bookshelf [online]. Available at: http://www.ncbi.nlm.nih.gov/books/NBK1421/. Accessed March 1, 2013.
4. Geschwind DH, Loginov M, Stern JM. Identification of a locus on chromosome 14q for idiopathic basal ganglia calcification (Fahr disease). Am J Hum Genet 1999;65:764–772.
5. Lemos RR, Oliveira DF, Zatz M, Oliveira JR. Population and computational analysis of the MGEA6 P521A variation as a risk factor for familial idiopathic basal ganglia calcification (Fahr's disease). J Mol Neurosci 2011;43:333–336.
6. Oliveira JR, Spiteri E, Sobrido MJ, et al. Genetic heterogeneity in familial idiopathic basal ganglia calcification (Fahr disease). Neurology 2004;63:2165–2167.
7. Volpato CB, De Grandi A, Buffone E, et al. 2q37 as a susceptibility locus for idiopathic basal ganglia calcification (IBGC) in a large South Tyrolean family. J Mol Neurosci 2009;39:346–353.
8. Dai X, Gao Y, Xu Z, et al. Identification of a novel genetic locus on chromosome 8p21.1-q11.23 for idiopathic basal ganglia calcification. Am J Med Genet B Neuropsychiatr Genet 2010;7:1305–1310.
9. Wang C, Li Y, Shi L, et al. Mutations in SLC20A2 link familial idiopathic basal ganglia calcification with phosphate homeostasis. Nat Genet 2012;44:254–256.
10. Hsu SC, Sears RL, Lemos RR, et al. Mutations in SLC20A2 are a major cause of familial idiopathic basal ganglia calcification. Neurogenetics 2013;14:11–22.
11. Zhang Y, Guo X, Wu A, et al. Association between a novel mutation in SLC20A2 and familial idiopathic basal ganglia calcification. PLoS One 2013;8:e57060.
12. Lemos RR, Oliveira MF, Oliveira JR. Reporting a new mutation at the SLC20A2 gene in familial idiopathic basal ganglia calcification. Eur J Neurol 2013;20:e43–e44.
13. Nicolas G, Pottier C, Maltête D, et al. Mutation of the PDGFRB gene as a cause of idiopathic basal ganglia calcification. Neurology 2013;80:181–187.
14. Chen WJ, Yao XP, Zhang QJ, et al. Novel SLC20A2 mutations identified in southern Chinese patients with idiopathic basal ganglia calcification. Gene 2013;529:159–162.
15. Keller A, Westenberger A, Sobrido MJ, et al. Mutations in the gene encoding PDGF-B cause brain calcifications in humans and mice. Nat Genet 2013;45:1077–1082.
16. Adzhubei IA, Schmidt S, Peshkin L. A method and server for predicting damaging missense mutations. Nat Methods 2010;7:248–249.
17. Kosaka K. Diffuse neurofibrillary tangles with calcification: a new presenile dementia. J Neurol Neurosurg Psychiatry 1994;57:594–596.
18. Yamada M, Asano T, Okamoto K, et al. High frequency of calcification in basal ganglia on brain computed tomography images in Japanese older adults. Geriatr Gerontol Int 2013;13:706–710.
19. Chung AJ, Cho G, Kim SJ. A case of paroxysmal kinesigenic dyskinesia in idiopathic bilateral striopallidodentate calcinosis. Seizure 2012;21:802–804.
20. Alemdar M, Selek A, Iseri P, Efendi H, Komsuoğlu SS. Fahr's disease presenting with paroxysmal non-kinesigenic dyskinesia: a case report. Parkinsonism Relat Disord 2008;14:69–71.
21. Chen WJ, Lin Y, Xiong ZQ, et al. Exome sequencing identifies truncating mutations in PRRT2 that cause paroxysmal kinesigenic dyskinesia. Nat Genet 2011;43;1252–1255.
22. Fabbri M, Marini C, Bisulli F, et al. Clinical and polygraphic study of familial paroxysmal kinesigenic dyskinesia with PRRT2 mutation. Epileptic Disord 2013;15:123–127.
23. Lederer E, Miyamoto K. Clinical consequences of mutations in sodium phosphate cotransporters. Clin J Am Soc Nephrol 2012;7:1179–1187.
24. Feild JA, Zhang L, Brun KA, Brooks DP, Edwards RM. Cloning and functional characterization of a sodium-dependent prostate transporter expressed in human lung and small intestine. Biochem Biophys Res Commun 1999;258:578–582.
25. Huqun, Izumi S, Miyazawa H, et al. Mutations in the SLC34A2 gene are associated with pulmonary alveolar microlithiasis. Am J Respir Crit Care Med 2007;175:263–268.
26. Hozumi I, Kohmura A, Kimura A, et al. High levels of copper, zinc, iron and magnesium, but not calcium, in the cerebrospinal fluid of patients with Fahr's disease. Case Rep Neurol 2010;2:46–51.
27. Takagi M, Ozawa K, Yasuda H, et al. Decreased bioelements content in the hair of patients with Fahr's disease (idiopathic bilateral calcification in the brain). Biol Trace Elem Res 2013;159:9–13.
28. Inden M, Iriyama M, Takagi M, et al. Localization of type-III sodium-dependent phosphate transporter 2 in the mouse brain. Brain Res 2013;1531:75–83.
29. Andrae J, Gallini R, Betsholtz C. Role of platelet-derived growth factors in physiology and medicine. Genes Dev 2008;22:1276–1312.
30. Giachelli CM, Jono S, Shioi A, et al. Vascular calcification and inorganic phosphate. Am J Kidney Dis 2001;38(4 suppl 1):S34–S37.
31. Jensen N, Schrøder HD, Hejbøl EK, et al. Loss of function of Slc20a2 associated with familial idiopathic basal ganglia calcification in humans causes brain calcifications in mice. J Mol Neurosci 2013;51:994–999.

Original Investigation

Lower Motor Neuron Involvement in TAR DNA-Binding Protein of 43 kDa–Related Frontotemporal Lobar Degeneration and Amyotrophic Lateral Sclerosis

Yuichi Riku, MD; Hirohisa Watanabe, MD; Mari Yoshida, MD; Shinsui Tatsumi, MD; Maya Mimuro, MD; Yasushi Iwasaki, MD; Masahisa Katsuno, MD; Yohei Iguchi, MD; Michihito Masuda, MD; Jo Senda, MD; Shinsuke Ishigaki, MD; Tsuyoshi Udagawa, PhD; Gen Sobue, MD

IMPORTANCE TAR DNA-binding protein of 43 kDa (TDP-43) plays a major role in the pathogenesis of frontotemporal lobar degeneration (FTLD) and amyotrophic lateral sclerosis (ALS). Although a pathological continuity between FTLD and ALS has been suggested, the neuropathological changes of the lower motor neuron (LMN) systems have not been assessed in TDP-43–associated FTLD (FTLD-TDP), to our knowledge.

OBJECTIVE To investigate a pathological continuity between FTLD-TDP and ALS by comparing their respective neuropathological changes in the motor neuron system.

DESIGN AND SETTING A retrospective clinical medical record review and a semiquantitative neuropathological evaluation of the cranial motor nerve nuclei and spinal cord were conducted at autopsy. We included 43 patients with sporadic FTLD-TDP, type A, B, or C, from 269 consecutively autopsied patients with TDP-43 proteinopathy. Patients were categorized as having FTLD without ALS, FTLD-ALS (onset of FTLD symptoms/signs preceded those of ALS), or ALS-FTLD (onset of ALS symptoms/signs preceded those of FTLD).

MAIN OUTCOMES AND MEASURES Neuronal TDP-43 pathological changes and neuronal loss.

RESULTS Forty-three patients were included in the clinical analysis, and 29 from whom spinal cords were obtained were included in the neuropathological analysis. Survival time was significantly shorter in the FTLD-ALS and ALS-FTLD groups than in the FTLD without ALS group ($P < .001$). At neuropathological examination, 89% of patients in the FTLD without ALS group showed aggregations of TDP-43 in the spinal motor neurons. The LMN loss was most severe in ALS-FTLD, followed by FTLD-ALS and FTLD without ALS. All the patients with type A or C FTLD-TDP were included in the FTLD without ALS group, and all those with type B pathological changes were in the FTLD-ALS or the ALS-FTLD group. Lower motor neuron loss and TDP-43–positive skeinlike inclusions were observed in all pathological subtypes.

CONCLUSIONS AND RELEVANCE The LMN systems of FTLD-TDP frequently exhibit neuropathological changes corresponding to ALS. Thus, a pathological continuity between FTLD-TDP and ALS is supported at the level of the LMN system.

Supplemental content at jamaneurology.com

Author Affiliations: Department of Neurology, Nagoya University Graduate School of Medicine, Nagoya, Japan (Riku, Watanabe, Katsuno, Iguchi, Masuda, Senda, Ishigaki, Udagawa, Sobue); Institute for Medical Science of Aging, Aichi Medical University, Aichi, Japan (Yoshida, Tatsumi, Mimuro, Iwasaki).

Corresponding Author: Gen Sobue, MD, Department of Neurology, Nagoya University Graduate School of Medicine, Tsurumai 65, Showa-ku, Nagoya, Japan (sobueg@med.nagoya-u.ac.jp).

JAMA Neurol. 2014;71(2):172-179. doi:10.1001/jamaneurol.2013.5489
Published online December 30, 2013.

Frontotemporal lobar degeneration (FTLD) is a sporadic or familial neurodegenerative disease that clinically encompasses frontotemporal dementia, language disorder, and motor symptoms.[1] Immunohistochemical profiles show that approximately half of patients with FTLD present with tau-positive disease, but the other half primarily exhibit an accumulation of TAR DNA-binding protein of 43 kDa (TDP-43), referred to as FTLD-TDP.[2-5] Currently, the cortical TDP-43 pathological changes in sporadic FTLD-TDP are classified into 3 subtypes: A, B, and C.[6-8]

TAR DNA-binding protein of 43 kDa is also a major disease protein in amyotrophic lateral sclerosis (ALS), which is characterized by upper motor neuron and lower motor neuron (LMN) involvement.[9] The pathological features of LMN involvement in ALS include neuronal loss, gliosis, TDP-43-positive neuronal inclusions with skeinlike or round shapes and glial inclusions, and Bunina bodies.[10]

Some patients exhibit symptoms of both ALS and FTLD, and the cerebral cortices of patients with FTLD and ALS almost always show type B TDP-43 changes.[7,11-13] Thus, a pathological continuity between FTLD and ALS has been proposed based on brain TDP-43 pathological findings. Studies of the cerebral cortex, including the motor cortex, and subcortical gray matter have shown common TDP-43 pathological findings in FTLD, FTLD with ALS, and ALS.[12,14-17] However, the neuropathological features of LMN systems in FTLD-TDP have not been investigated comprehensively, particularly in the spinal cord, although characterization of these features is necessary to confirm the pathological relationship between FTLD and ALS.

In this study, we investigated LMN pathological findings in patients with sporadic FTLD-TDP who clinically demonstrated FTLD, FTLD with ALS, or ALS. We also investigated the correlation between TDP-43 pathological subtypes (type A, B, and C) and LMN involvement to further elucidate the continuity of FTLD and ALS.

Methods

Study Patients

We enrolled 269 consecutively autopsied patients with sporadic and adult-onset FTLD, FTLD with ALS, or ALS in which pathological aggregation of TDP-43 was confirmed at the Department of Neuropathology, Institute for Medical Science of Aging, Aichi Medical University, from 1988 to 2012. All patients had been clinically evaluated by neurological experts in the affiliated hospitals of Nagoya University School of Medicine or Aichi Medical University. Permission to perform an autopsy and archive the nervous system tissues for research purposes was obtained from family members after death. The clinical data on the included patients were obtained from case notes made at diagnosis and at an advanced stage of illness. We initially excluded 216 of the 269 patients because they did not present clinical FTLD symptoms. In 53 patients, FTLD or FTLD with ALS was diagnosed according to the diagnostic criteria of FTLD and ALS.[1,18] Moreover, we subclassified FTLD with ALS into FTLD-ALS (onset of FTLD symptoms/signs preceded those of ALS) and ALS-FTLD (onset of ALS symptoms/signs preceded those of FTLD) groups.

The enrolled patients were categorized into 3 groups: FTLD without ALS, FTLD-ALS, and ALS-FTLD. The FTLD symptoms were categorized into 2 groups: behavior-variant frontotemporal dementia and language impairments.[14] The LMN symptoms/signs were defined by progressive muscular weakness, muscular atrophy, fasciculation, or electromyographic findings. We excluded patients with Alzheimer disease-associated neurofibrillary pathological abnormalities that were more advanced than Braak stage IV,[19] those with argyrophilic grain disease, and those with invalid clinical data. Finally, 43 patients were included in the clinical analysis (11 with FTLD without ALS, 9 with FTLD-ALS, and 23 with ALS-FTLD). For comparison, we prepared 13 age-matched controls (mean [SD] age at death, 68.2 [6.9] years) who had no diagnosis of any neurodegenerative disease, dementia, or cerebrovascular disease.

Clinical Analyses

The information regarding sex, age at onset, disease duration, and duration between onset of FTLD and ALS was collected from clinical notes. Causes of death were classified as respiratory failure due to respiratory muscle weakness, pneumonia, or other. The last category comprised systemic diseases other than respiratory failure or pneumonia, including cancer, ileus, infections, and renal failure. Information on the subtypes of dementia, clinical data on motor symptoms, and electromyographic results were also collected.

Pathological Evaluations

For the neuropathological analysis, we excluded patients who had received a respirator/tracheotomy (n = 11) or whose spinal cord was not available (n = 3). In total, 29 patients were included in the neuropathological analysis and divided into 3 groups: FTLD without ALS (n = 9), FTLD-ALS (n = 8), and ALS-FTLD (n = 12). The tissues were fixed in 20% neutral-buffered formalin. The paraffin-embedded tissue blocks were cut at a thickness of 4.5 μm. We evaluated sections from the spinal cord and whole brain. The whole spinal cord was examined at each segmental level, but only the cervical cord was available in 3 patients and the sacral cord was not available in another 3.

For routine neuropathological examinations, the sections were stained with hematoxylin-eosin and Klüver-Barrera. Immunohistochemical studies were performed using a standard polymer-based method with the EnVision Kit or anti-goat immunoglobulin (Dako). As primary antibodies, we used antibodies to the following: anti-ubiquitin (ubiquitin, monoclonal mouse, 1:250; Millipore), anti-TDP-43 (TARDBP, polyclonal rabbit, 1:2500; ProteinTech), anti-phosphorylated TDP-43 (pTDP-43 ser409/410, polyclonal rabbit, 1:2500; CosmoBio), anti-phosphorylated tau (AT-8, monoclonal mouse, 1:4000; Innogenetics), anti-β-amyloid (β-amyloid 6F/3D, monoclonal mouse, 1:100; Dako), anti-CD68 (CD68, monoclonal mouse, 1:200; Dako), anti-cystatin C (cystatin C, polyclonal rabbit, 1:200; Dako), p62 N-terminal (p62N, polyclonal

guinea pig, 1:100; Progen), anti-ubiquilin 2 (UBQLN-2 5F5, monoclonal mouse, 1:5000; Abnova), and anti-choline acetyltransferase (ChAT, polyclonal goat, 1:100; Millipore). Diaminobenzidine (Wako) was used as the chromogen.

Antigens were retrieved with trypsin for anti-CD68 immunohistochemistry and with 95°C 3 mmol/L citrate buffer at 95°C for 20 minutes, followed by 5-minute incubation in 98% formic acid for anti-p62N, anti-TDP-43, anti-pTDP-43, and anti-ChAT immunohistochemistry. To confirm the presence of TDP-43-positive inclusions within the cholinergic motor neurons, we performed double immunohistochemistry using anti-pTDP-43 and anti-ChAT antibodies. Spinal cord specimens were prepared from 3 patients with type A, 3 with type B, and 2 with type C. Initially, the specimens were immunostained with the anti-ChAT and anti-goat immunoglobulin antibodies and diaminobenzidine. The anti-ChAT antibody was inactivated in distilled water at 100°C for 20 minutes, followed by immunohistochemistry with pTDP-43 and violet pigmentation using a VIP Peroxidase Substrate Kit (SK-4600; Vector).

For the semiquantitative neuropathological analysis, 2 investigators (Y.R. and M.Y.) observed the specimens containing the facial and hypoglossal nuclei and the anterior horn of the spinal cord. They evaluated the severity of LMN neuropathological changes that are indicative of ALS (neuronal loss, gliosis, aggregation of macrophages, TDP-43-immunopositive neuronal inclusions, and Bunina bodies) and graded neuronal loss and gliosis using Klüver-Barrera and hematoxylin-eosin staining. The investigators also evaluated the aggregations of macrophages rather than rod-shaped microglia using anti-CD68 immunohistochemistry and identified Bunina bodies using hematoxylin-eosin staining and anti-cystatin C immunohistochemistry. They scored the severity of neuronal loss and gliosis as grade 0 (none), 1 (mild), 2 (moderate), or 3 (severe) (eFigure 1 in Supplement. The appearance of TDP-43-positive inclusions was scored as grade 0 (none), grade 1 (1-5 neuronal inclusions per 5 fields; ×20 objective), grade 2 (6-10 inclusions), or grade 3 (≥11 inclusions) using anti-pTDP-43 immunohistochemistry.

Pathological cortical TDP-43 subtypes were identified according to current neuropathological criteria, using specimens from the frontal lobes, temporal lobes, and hippocampus.[5] For FTLD-TDP, type A was defined as the presence of neuronal cytoplasmic inclusions predominantly in the neocortex layer 2 and short dystrophic neurites; type B, as a predominance of neuronal cytoplasmic inclusions in all cortical layers; and type C, as a predominance of long dystrophic neurites in layer 2 and cytoplasmic inclusions in the dentate granular cells of the hippocampus. Our patient series did not include type D, which is characterized by numerous short dystrophic neurites and neuronal intranuclear inclusions in association with valosin-containing protein gene mutations. We also evaluated pathological changes in the upper motor neuron systems that include the primary motor cortex and corticospinal tract (CST). We evaluated the presence or absence of neuronal loss and gliosis in the primary motor cortex and myelin pallor, as well as the aggregation of macrophages in the CST.

Immunohistochemical Screening of Hexanucleotide Repeat Expansion Sequence in Chromosome 9 Open Reading Frame 72

Our study focused on sporadic FTLD-TDP, and patients with familial histories of FTLD or ALS, dementia, or other neurodegenerative diseases were excluded. However, FTLD or ALS associated with chromosome 9 open reading frame 72 (C9ORF72) hexanucleotide expansion exhibits pathological aggregation of TDP-43 and, in some cases, low penetration,[20,21] although these mutations are extremely rare in Japan.[22] It was recently reported that the pattern of ubiquilin abnormalities in ALS and FTLD corresponds well with the presence of C9ORF72 hexanucleotide expansion.[23] The UBQLN-2-positive, p62-positive, but TDP-43-negative thick dystrophic neurites are abundantly present in patients with C9ORF72 hexanucleotide expansion, predominantly in the hippocampus and cerebellum. Because the materials for a genetic study were not available for a large proportion of our patients, we histologically screened C9ORF72 hexanucleotide expansion with the absence of UBQLN-2 and p62N-positive thick dystrophic neurites in the temporal lobes and cerebella of all patients.

Statistical Analysis

The Mann-Whitney test was applied to continuous variables between 2 groups, and the Kruskal-Wallis test was applied to the analysis of continuous variables among 3 groups. The χ^2 test was used for categorized variables among 3 groups. Spearman rank correlation coefficient analyses were applied to univariate correlations between the clinical groups and severity of pathological changes. Survival curves were constructed using the Kaplan-Meier method. The end point of clinical course was defined as death or the introduction of a respirator or tracheotomy. The significance level for all comparisons was set *at* $P < .05$. All statistical tests were 2 sided and were conducted using the PASW 18.0 program (IBM SPSS).

Results

Clinical Analysis

Patient characteristics are summarized in the **Table.** The mean (SD) time from symptom onset to death or respirator or tracheotomy administration was 50.5 (58.4) months across all patients. The survival time from symptom onset did not differ significantly between the FTLD-ALS and ALS-FTLD groups but was significantly shorter for the FTLD without ALS group than for the FTLD-ALS or ALS-FTLD group (**Figure 1** and Table; $P < .001$). The most common cause of death for the ALS-FTLD and FTLD-ALS groups was respiratory failure, but patients with FTLD without ALS commonly died of other systemic diseases ($P < .001$). Frequencies of dementia subtypes did not significantly differ between the clinical groups.

With regard to motor symptoms/signs, 3 patients in the FTLD without ALS group had hyperreflexia, 1 had the Babinski sign, and 1 had spasticity, but none had a clinical diagnosis of progressive lateral sclerosis (PLS) according to the published diagnostic criteria of PLS.[24] Patients with FTLD-ALS or